Astron. Astrophys. 335, 929–942 (1998)

ASTRONOMY AND ASTROPHYSICS

CCD photometry of M 80 and the ranking of the C-M diagrams of galactic globulars

E. Brocato[1], **V. Castellani**[1,2,3], **G.A. Scotti**[2], **I. Saviane**[4], **G. Piotto**[4], **and F.R. Ferraro**[5]

[1] Osservatorio Astronomico di Collurania, Via M. Maggini, I-64100 Teramo, Italy (brocato,vittorio@astrte.te.astro.it)
[2] Dipartimento di Fisica, Università di Pisa, Piazza Torricelli 2, I-56100 Pisa, Italy (giovanni@astr1pi.difi.unipi.it)
[3] Istituto Nazionale di Fisica Nucleare, LNGS, I-67100 L'Aquila, Italy
[4] Dipartimento di Astronomia, Università di Padova, Italy (saviane,piotto@pd.astro.it)
[5] Osservatorio Astronomico, Via Zamboni 33, I-40126 Bologna, Italy (ferraro@astbo3.bo.astro.it)

Received 24 November 1997 / Accepted 19 March 1998

Abstract. We present deep B and V CCD photometry of the intermediate metallicity, high central density galactic globular cluster M 80. More than 10000 stars have been measured, reaching a limiting magnitude $V \simeq 23$. The color magnitude diagram shows a population of very hot horizontal branch (HB) stars, stretching down to V magnitudes fainter than those of the turn off stars, to the limiting level of the present photometry. Using the giant branch as metallicity indicator, we derive [Fe/H]$= -1.71 \pm 0.20$. From the location of the HB, we obtain an apparent distance modulus (m-M)$_V = 15.58 \pm 0.12$. The R ratio gives Y=0.25 ± 0.05 and shows a radial trend, with the HB stars in the blue tail more concentrated than the red giant stars. We show also evidences that the hot HB stars are "bona fide" normal He burning stars.
The color–magnitude diagram of M 80 has been compared with the corresponding diagrams of other clusters with similar metallicity (within ± 0.1 dex), and with different metallicity. Both comparisons reveal clear differences, which might be interpreted as uncertainties in color calibrations of the color-magnitude diagrams or might reflect differences in the "global" metallicity of the galactic globular clusters.

Key words: globular clusters: individual: NGC 6093 – stars: evolution – Hertzsprung–Russell (HR) diagram – stars: Population II – stars: horizontal-branch

1. Introduction

NGC 6093 (M 80) is a bright, moderately metal poor globular cluster in the southern hemisphere for which only old photographic photometry for the more luminous cluster stars is available to date (Harris & Racine 1974, hereafter HR74). However, the cluster appears to be an interesting object in many respects. As a first point, the estimated metallicity [Fe/H] = -1.68 (Zinn and West 1984) appears very similar to the cluster M 3 ([Fe/H]= -1.65, Zinn and West 1984) [1]. In spite of this similarity, the two clusters have quite different Horizontal Branch (HB) morphology, with M 80 closely resembling M 13-like clusters where HB stars are essentially confined to the blue side of the RR Lyrae instability region. Thus M 80 appears a cluster where the "second parameter" affecting the HB distribution in galactic globular clusters (GGC) can be investigated.

Our interest in this cluster is furtherly increased by the evidence that M 80 is one of the densest globular clusters in the Galaxy, with an estimated central density as large as $\log \rho(M_\odot/pc^3)$=5.68 (Djorgovski 1993). Indeed, there are increasing evidences for which high central density GGCs appear correlated with the occurrence of a peculiar population of very hot HB stars, forming a HB "blue tail" extended to very large effective temperatures (see e.g. Buonanno et al. 1985, Djorgovski & Piotto 1993, Fusi Pecci et al. 1993, Castellani 1994, Buonanno et al. 1997). Moreover, a very blue HB morphology for M 80 was already predicted on the basis of high ultraviolet emissions observed with IUE spectra (Caloi et al. 1980, 1984) and has been recently confirmed by high resolution HST observations presented by Shara and Drissen (1995). According to this scenario, M 80 appears an ideal target to investigate the quoted correlation.

In this paper we present the results of such an investigation. In the next section, observations and data reduction will be presented. In Sect. 3 we present the color–magnitude diagram (CMD), and discuss all the parameters which can be derived from it. Sect. 4 will be devoted to the luminosity function and to a comparison with theoretical models. Population ratios and population gradients will be presented in Sect. 5 together with a short discussion on the possible origin of the blue HB tail. Sect. 6 will deal with a discussion on the CMD morphology. We will show the comparison with a sample of clusters with similar metallicities, discussing at the light of present theoretical knowledge the possible origin of some puzzling differences. The discussion will be finally extended to the CMDs of a large

Send offprint requests to: E. Brocato

[1] note that both clusters will result more metal rich ([Fe/H]=-1.3) in the metallicity scale by Carretta and Gratton (1997)

Table 1. For each field and each filter the Table shows the number of frames (N), the exposure time (t) and the seeing for the best frame.

field	filter	N	t (sec)	seeing (arcsec)
C	V	3	42	1.1
C	B	3	122	1.1
SW	V	3	150	0.9
SW	B	3	300	1.1
NW	V	3	150	0.9
NW	B	3	302	1.1
NE	V	3	100	0.9
NE	B	1	150	1.2
SE	V	3	150	1.2
SE	B	1	150	1.2
OFF	V	1	900	1.2
OFF	B	1	1200	1.1
EXT	V	1	480	1.1
EXT	B	1	600	1.0

sample of GGCs, disclosing unexpected evidences which might suggest a possible revision of the present evaluation of the ranking in metallicity of GGCs.

2. Observations and data reduction

Observations were carried out during the nights July 15 and 16, 1993, at the ESO 3.58 NTT equipped with EMMI. A set of 17 CCD B–frames was secured with the Tektronix TK1024 (ESO #31) using filter ESO#603 at EMMI blue arm. 13 CCD V–frames were obtained with LORAL2048 detector (ESO #34) and filter ESO#606 at EMMI red arm. Six fields, partially overlapping, covering a total area of about 12×12 arcmin^2, grossly centered on the cluster, were observed in good seeing conditions (FWHM 0.9-1.2 arcsec). An additional field centered at ~ 30 arcmin from the cluster center (~ 2 tidal radii) was observed in order to estimate the field star contamination. The details of the exposures are given in Table 1. Flat-field and bias images were taken at the beginning and at the end of each night to correct for the detector response to uniform sensitivity.

Data reduction was performed using the package ROMAFOT (Buonanno et al. 1979, 1983) for crowded field photometry. Standard procedures to determine the PSF, to group and to fit the objects were adopted (see Ferraro et al. 1990 for a description). For each field the master list was created from the individual frame photometry after interactively checking those objects for which the goodness of fit estimators assumed anomalous values. A total number of 10176 single stars was detected and measured in both B and V–bands, once the entire reduction procedure had been fully performed. The threshold values adopted in the search phase were fixed according to the crowding conditions and exposure times, on the basis of several tests, in order to limit the number of spurious detections. Information about the threshold values adopted and the number of objects detected for each field are shown in Table 2.

Due to non photometric sky conditions, the observation of photoelectric primary standards outside the M 80 field did not allow a reliable calibration. In order to calibrate our data we used a set of 141 stars in common with Saviane & Piotto (1998) covering the ranges $-0.30 < B - V < 1.35$ and $13.5 < V < 17.5$. The following relations have been obtained:

$$B = b + (0.10 \pm 0.01)(b - v) + const.$$

$$V = v + (0.02 \pm 0.01)(b - v) + const.$$

where B and V are the magnitude listed by Saviane & Piotto, and b and v the instrumental ones. The former have been calibrated using a set of 12 standard stars from Landolt (1992); the uncertainty on the calibrated magnitudes quoted by Saviane & Piotto is 0.03 magnitudes in V and 0.04 magnitudes in (B-V). All the cluster fields are partially overlapping, so the common stars have been used to calibrate to the same instrumental magnitudes. Unfortunately, the background field do not overlap with any cluster fields. In this case the calibration has been performed by using, as secondary standards, the stars measured in the cluster frames obtained just before and after the exposures on the background field.

Table 2. For each field the Table shows the threshold adopted in the ROMAFOT/search procedure (Thr.) expressed in units of sky Poisson noise (σ_{sky}) and the number of stars detected.

field	Thr. $\times\sigma_{sky}$	N_{stars}
C ($r < 100$ pix)	150	354
C ($r > 100$ pix)	12	6366
NW	14	1120
SW	14	1362
SE	14	1185
NE	7	548
OFF	7	1328
EXT	7	727

The constants present a dispersion of 0.06 and 0.05 mag in B and V, respectively.

The CMD for all the detected stars with a distance from the cluster center $r > 100$ px (pixel size 0.35 arcsec) is shown in Fig. 1. The data of the present investigation can be usefully compared with the photographic data presented by HR74. Lacking a finding chart for stars measured in 1974, we simply selected in our sample the stars in the same region covered by HR74 (100 arcsec $< r <$ 250 arcsec), plotting the corresponding CMDs. Even if the HR74 data are affected by a larger internal photometric error, one finds that the CMD morphologies for the two dataset overlap quite satisfactorily.

The internal accuracy of our CCD measurements has been estimated on the basis of the *rms* frame-to-frame scatter of the instrumental magnitudes for each individual star, computed as in Ferraro et al. (1990). The mean internal errors are, approximately, $< \sigma_V > \simeq 0.007$ and $< \sigma_{B-V} > \simeq 0.010$ for $12 < V < 18$; $< \sigma_V > \simeq 0.017$ and $< \sigma_{B-V} > \simeq 0.025$ for $18 < V < 21.5$.

The final photometric error includes also the error involved in the calibration procedure and the uncertainties related to the various transformations. We estimate that systematic total errors

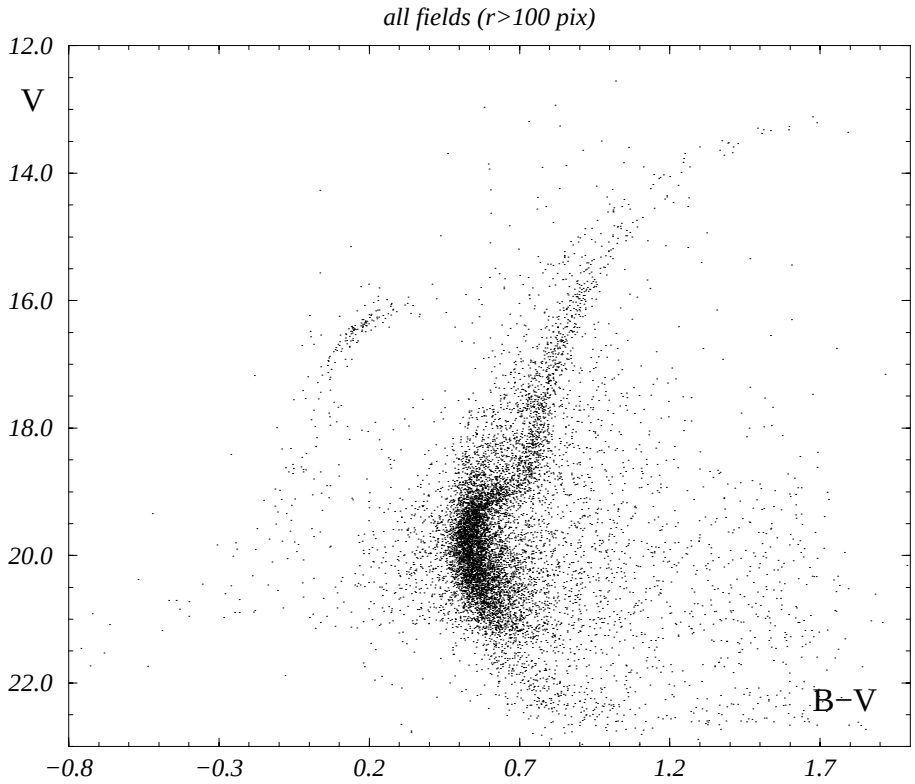

Fig. 1. CMD for all fields, only star with $r > 100$ (9822 objects).

up to 0.05 mag in V and 0.08 mag in $B-V$ cannot be ruled out in our measurements, at least for very blue and/or very red stars.

Nevertheless, our data and the photographic measurements by HR74 do not show significant zero point differences. In particular, there is a good agreement in the two color scales: they found $(B-V)_g = 0.92$ as mean red giant branch (RGB) color at the magnitude $V_{RR} = 15.90$, while we obtain $(B-V) = 0.90$ at the same magnitude level from our CMD (see next section for a detailed discussion on the magnitude of the HB and the color of the base of the giant branch).

For what concerns the completeness of our sample, we made several tests following the procedure described in Ferraro et al. (1990): we randomly added to the original frame a group of stars of known magnitude (N_{add}), re-reduced the frame and calculated the ratio $F = N_{rec}/N_{add}$ which represents the degree of completeness, where N_{rec} is the number of artificial stars retrieved. We performed the tests in four annuli at different distances from the cluster center, in order to account for the varying crowding conditions.

As shown by the artificial star experiments, the sample with $V < 20$ mag is fairly complete (i.e. $F > 90\%$) down to 250 pix from the cluster center ($\simeq 90$ arcsec). Therefore, where in the following we make use of star counts (luminosity function, R parameter), we refer only to this subsample.

3. The color-magnitude diagram

Table 3 presents the values adopted as fiducial points for the CMD of M 80 obtained as follows:

Table 3. Fiducial points for M 80.

V	$B-V$	V	$B-V$
MS+SGB+RGB		19.700	0.521
13.200	1.680	19.900	0.526
13.310	1.590	20.100	0.531
13.610	1.430	20.300	0.548
13.960	1.290	20.500	0.555
14.400	1.165	21.050	0.613
14.800	1.070	21.550	0.677
15.200	0.993	22.050	0.762
15.600	0.933	22.550	0.913
16.000	0.893		
16.400	0.858	HB	
16.800	0.826	16.147	0.320
17.200	0.796	16.352	0.220
17.600	0.774	16.569	0.139
18.000	0.755	17.000	0.080
18.400	0.730	17.500	0.026
18.800	0.700	18.000	0.023
19.010	0.635	18.500	0.000
19.100	0.589	19.000	-0.023
19.300	0.553	19.500	-0.057
19.500	0.536	20.000	-0.108

i) *H–burning CMD sequences.* In the range $19.0 < V < 23.0$ mag we selected stars with $r > 300$ pix from the cluster center (to reduce the number of spurious blended objects), binned the data in magnitude (0.5, 0.2 mag bins, for the main sequence (MS) and the TO/subgiant branch, respectively) and, for each bin, calculated the mean V and the mode of the (B-V)

histogram (0.02 mag bins); for $14.2 < V < 19.0$ mag, we used the same method but dealing with data with $r > 100$ pix and V–bins of 0.4 mag. For the upper part of the RGB (V<14.2 mag) the 3 brighter fiducial points were determined by eye estimation.

ii) *HB.* We used data from the whole sample; in the range $16.75 < V < 20.50$ mag we binned by 0.5 mag in V (0.1 mag in color), taking the mean V, B-V for each bin.

The TO appears rather well defined in shape, together with the subgiant (SG) and the initial portion of the red giant branch. The same figure shows that the expectation about the HB population is fully confirmed by the present observations: below the already known blue HB there is a well defined population of very hot HB stars stretching down to V-magnitudes fainter than those of TO stars. Recalling that the decrease in V-magnitude is mainly the consequence of bolometric correction, this is an evidence of the large temperatures reached by these HB stars. Quantitative evaluation based on theoretical models for hot HB stars (Castellani et al. 1995) and Kurucz (1992) atmosphere models indicates that the bottom of the cluster "blue tail" (hereafter BT) should be populated by stars as hot as $\log T_e \simeq 4.40$, that is by stars where the He core is surrounded by a H rich envelope with mass of the order of just $\simeq 0.01 M_{\odot}$.

According to a well established scenario, the location of the RGB can be first used to derive and/or to test information about the cluster metallicity, since the RGB becomes bluer and steeper as the metallicity decreases. Several evaluations of the cluster metallicity are already available in the literature. Zinn (1985) gives for M 80 a value [Fe/H] $= -1.68$. Suntzeff et al. (1991) adopt a value of -1.64 based on the system of Zinn & West (1984). [Fe/H] $= -1.55$ is derived by Bica & Pastoriza (1983) from DDO photometry, while Brodie & Hanes (1986) give [Fe/H] $= -1.57$ from a low-resolution spectrophotometric study. The mean value from the above metallicity determinations is [Fe/H] $= -1.61 \pm 0.06$ (*rms* error); taking into account the typical ~ 0.2 dex uncertainty on the metallicity scales (Zinn and West 1984), we have [Fe/H]$=-1.6 \pm 0.2$.

"Photometric" estimates of the cluster metallicity can be derived from several RGB–based parameters calibrated in terms of [Fe/H]. In the following we will make use of the parameters $(B-V)_{0,g}$ (Sandage & Smith 1966), $\Delta V_{1.4}$ (Sandage & Wallerstein 1960) and S (Hartwick 1968). However, in order to evaluate a correct value for these parameters one needs information on both the interstellar reddening $E(B-V)$ and the zero age horizontal branch (ZAHB) luminosity level at the temperature of the RR Lyrae gap: V_{HB}. These two quantities have been estimated as follows:

i) $E(B-V)$. HR74 determined a color excess for M 80 of 0.16 ± 0.03 from the comparison of their CMD with the mean lines of M 13. Racine (1973) found a value of 0.17 based on the cluster's integrated spectral type. More recently, using the same method, Reed et al. (1988) obtained a value of 0.18. In the following we will adopt $E(B-V) = 0.17 \pm 0.03$ and comment on the possible effect of the uncertainties in the reddening on other derived quantities.

Table 4. Metallicity from RGB parameters: relations and derived values for M 80.

Relation	References	Derived [Fe/H]
	$(B-V)_{0,g}$	
$4.30(B-V)_{0,g} - 5.00$	Zinn & West 1984	-2.08 ± 0.43
$3.84(B-V)_{0,g} - 4.63$	Gratton 1987	-2.02 ± 0.38
$4.68(B-V)_{0,g} - 5.19$	Costar & Smith 1988	-2.01 ± 0.47
$2.85(B-V)_{0,g} - 3.76$	Gratton & Ortolani 1989	-1.82 ± 0.28
	$\Delta V_{1.4}$	
$-0.924\Delta V_{1.4} + 0.913$	Zinn & West 1984	-1.77 ± 0.14
$-1.01\Delta V_{1.4} + 1.30$	Costar & Smith 1988	-1.63 ± 0.15
$-0.65\Delta V_{1.4} + 0.28$	Gratton & Ortolani 1989	-1.61 ± 0.10
	S	
$-0.46S + 0.62$	Ferraro et al. 1991	-1.68 ± 0.64
$-0.29S + 0.01$	Gratton & Ortolani 1989	-1.44 ± 0.41

ii) V_{HB}. Due to the reduced number of RR Lyrae variables (only six stars), the measurement of the ZAHB level is rather difficult in this cluster. Moreover, because of the blue HB morphology, these variables are probably evolved HB stars and do not represent the ZAHB level correctly. In order to derive V_{HB}, we have overplotted, on the horizontal branch of M 80, the HB of two other clusters: M 5 (Carney et al. 1991) and M 15 (Durrell & Harris 1993). These clusters have sufficiently populated HBs both in the blue side and in the instability strip; Fig. 2 shows the two superimpositions. Note that these clusters have either higher (M 5) or lower (M 15) metallicities than M 80, but this does not affect our determination of the HB luminosity. Following this procedure we got $V_{HB} = 16.20 \pm 0.10$ in both cases. This value is slightly fainter than $V_{RR} = 15.89$ and $V_{RR} = 15.90$ given, respectively, by Wehlau et al. (1990) and HR74 from the mean magnitude of RR Lyrae stars in M 80, confirming the probable existence of evolutionary effects in these variables.

The color of the RGB at $V = 16.2$ is $(B-V)_g = 0.85 \pm 0.05$, where the error includes the uncertainty on the HB level, to which we have to add an uncertainty of ~ 0.08 mag due to the photometric error (*cf. Sect. 2*). The true RGB color is then $(B-V)_{0,g} = 0.68 \pm 0.10$ where the uncertainty includes also the error on $E(B-V)$.

Inserting this value in the relations listed in Table 4 we obtain the corresponding values for [Fe/H] showed in column 3 of the same Table: a weighted mean gives [Fe/H] = -1.94 ± 0.13.

The V magnitude of the RGB at $(B-V) = 1.4 + E(B-V)$ is $V_{1.4}$ = 13.3 $\pm$0.1; the error due to the uncertainty in the reddening has a negligible effect, compared to the ~ 0.1 mag uncertainty in defining the RGB ridge line. Therefore, $\Delta V_{1.4} = 2.90 \pm 0.15$: the relations in Table 4 lead to the metallicity values listed in column 3, and a weighted mean gives [Fe/H] = -1.65 ± 0.09.

Finally, we can use the parameter $S = 2.5/\Delta(B-V)_{2.5}$, where $\Delta(B-V)_{2.5}$ is the difference between $(B-V)_g$ and the

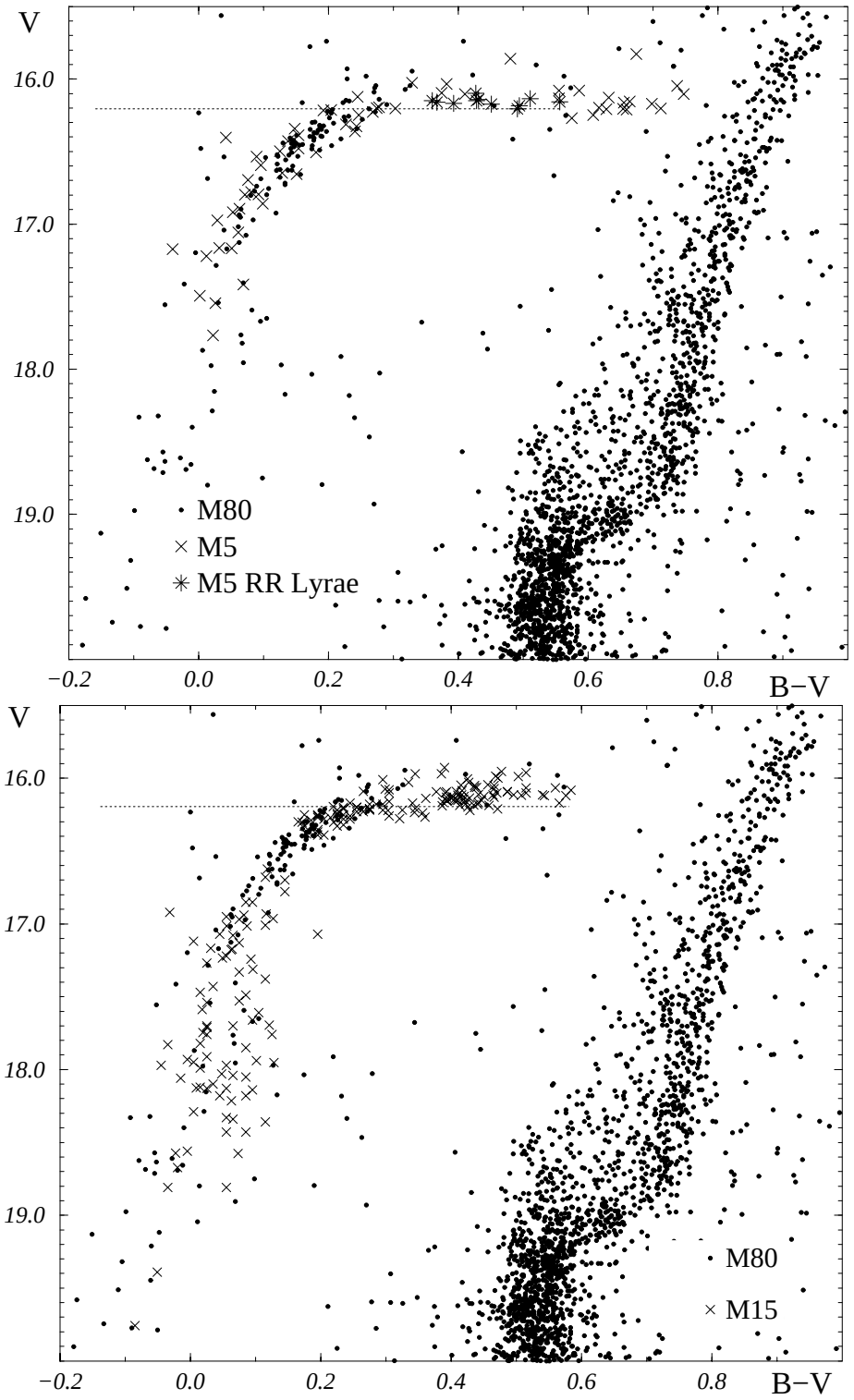

Fig. 2. The HBs of M 5 (upper panel) and of M 15 (lower panel) are superimposed on M 80 CMD. M 5 and M 15 CMDs have been shifted, respectively, by $\Delta V = +1.10$, $\Delta(B-V) = +0.13$ and $\Delta V = +0.35$, $\Delta(B-V) = +0.06$. The dotted line represents the ZAHB level.

color of the RGB point which is 2.5 V mag brighter than the HB. Therefore, $S = (2.5 \pm 0.15)/(0.5 \pm 0.07) = 5 \pm 1$, where the errors include both the uncertainty in locating the two points on the ridge lines, and the photometric errors. A weighted mean of the values listed in Table 4 finally gives [Fe/H] = -1.51 ± 0.17.

In summary, we have now three additional determinations of [Fe/H]. We must point out that the first two photometric methods rely on the assumed reddening and that increasing the reddening would increase the estimated metallicity. In this respect, it might be of some interest to note that the [Fe/H] value derived from the S index, which does not depend on the cluster reddening, is very close to the mean value derived from the literature. In any case, a weighted mean of the three metallicity determinations gives [Fe/H] = -1.71 ± 0.20.

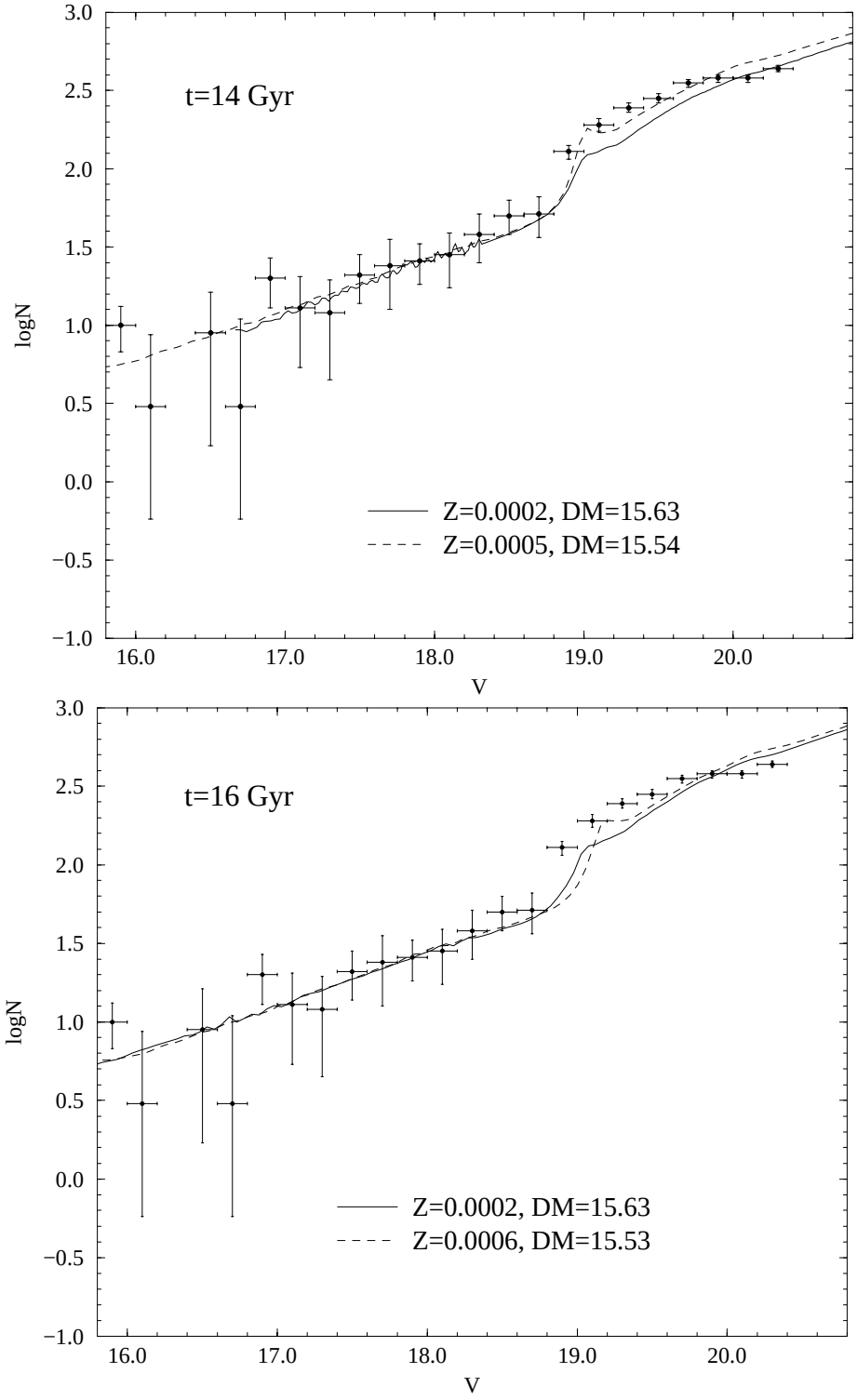

Fig. 3. Observed luminosity function (filled circles) for the stars with $r > 250$ pix not belonging to the NE field and lying within $\pm 3\sigma_{B-V}$ from the cluster ridge line, decontaminated for the field stars contribution. The vertical error bars represent the Poisson standard deviation, the horizontal ones account of the uncertainty in the V_{HB} determination (± 0.10 mag). Theoretical LF, from Degl'Innocenti et al. (1996), are computed for the specified ages and metallicities, shifted by the labeled DM.

However, even regarding the quoted error as at 3σ level, one has to notice that the quoted metallicity determination is far from being very satisfactory, since it leaves room for the cluster being regarded either as a very metal poor (Z=0.0002) or a moderately metal rich (Z=0.0006) object.

By relying on the above estimates one can proceed to a comparison with current evolutionary theories. According to Caputo (1997), theoretical results from Castellani et al. (1991: CCP) can be combined with Kurucz (1992) atmosphere models to derive the ZAHB luminosity

$$M_V = 1.45 + 0.21 \log Z$$

which gives, for the assumed metallicity, $M_{\rm v} = 0.74 \pm 0.05$. However, recent improvements in the input physics (see Salaris,

Degl'Innocenti & Weiss 1997) already disclosed that CCP probably underestimated the HB luminosity by $\Delta M_V \simeq 0.1$. With such a correction, from the observed magnitude of the HB, one finally derives a cluster apparent distance modulus (m-M)$_V = 15.56 \pm 0.15$.

Apart from the theoretical route, we could obtain a distance modulus estimate using other empirical or semi–empirical calibrations of the $M_V(ZAHB)$ vs. [Fe/H] relation. Column 1 of Table 5 summarizes the different values of the absolute magnitude of the ZAHB using the most recent calibrations of the relation. The corresponding distance modulus (and uncertainties) are in column 3 (and 4, respectively) of Table 5. A mean of the different distance moduli in Table 5 gives: (m-M)$_V = 15.58 \pm 0.12$, very similar to the value obtained above from the theoretical HB magnitude. Assuming E(B-V)=0.17, and A$_V$=3E(B-V) we get an absolute distance modulus: (m-M)$_0$=15.07$\pm$0.16

4. The luminosity function

Making reference to this (m-M)$_0$ value and bearing in mind the above evaluation of the cluster distance modulus one can further compare the observed sample of RGB stars with the theoretical prescriptions.

In the upper panel of Fig. 3 the RGB luminosity function (LF) is compared with the theoretical LF for the two labeled choices of the metallicity and for a cluster age t=14 Gyr (t=16 Gyr in the lower panel). The observed LF is obtained selecting stars with $r > 250$ pix, not belonging to the NE field (because of the lower exposure time of the NE V–frame) and lying within $\pm 3\sigma_{B-V}$ from the cluster ridge line. The LF is also corrected for the field stars contamination by using the CMD obtained in the external region, located ~ 30 arcmin from the cluster center. Theoretical LFs (Degl'Innocenti et al. 1997) are normalized to the total number of stars on the RGB ($V < 18.5$ mag). The last two points ($V > 20$ mag) of the observed LF in Fig. 3 are clearly below the theoretical LF, this could be due to the assumed IMF but it is very likely due to the incompleteness of the sample at these fainter magnitudes (*cf. Sect. 2*).

The overall morphology would suggest that the upper limit of the adopted metallicity range should be preferred to account for the star distribution around the subgiant branch (i.e. around $V \simeq 19$). Comparison between the upper and lower panel of the figure shows that, under the above quoted assumptions, models for an age of 14 Gyr better reproduce the observed LF. As shown in Fig. 4, the LF also allows to locate the position of the RGB luminosity bump marking the encounter of the H burning shell with the interior chemical discontinuity. As shown by Fusi Pecci et al. (1990), the bump is better revealed by the changing slope of the cumulative luminosity function produced by the variation in the core mass-luminosity relation for the RGB structures. The bottom panel of Fig. 4 shows that the bump can be recognized in the usual differential luminosity function too. We find $V_{bump} = 15.95 \pm 0.05$. The position of the bump in M 80 can now be compared with the results obtained for the other globular clusters: Fusi Pecci et al. (1990) defined the parameter

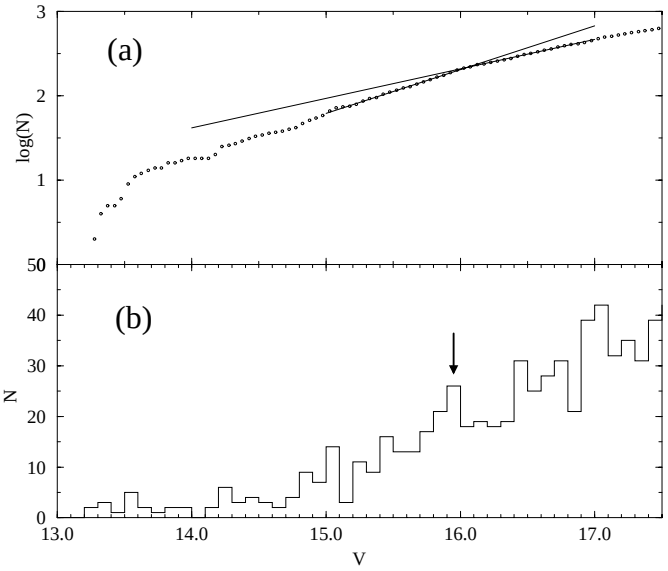

Fig. 4a and b. Cumulative (**a**) and differential (**b**) luminosity function for all the stars detected brighter than 17.5 mag.

$\Delta V_{\rm HB}^{\rm bump} = V_{\rm bump} - V_{\rm HB}$ and studied its dependence on the cluster metallicity. The authors replaced [Fe/H] with the parameter $s(Z)$ (cf. their definition), which was useful in order to make the comparison with the theoretical models. From the previous discussion, for M 80 we have $\Delta V_{\rm HB}^{\rm bump} = -0.25 \pm 0.11$. M 80 shares the general trend of the present sample of clusters (cf. Saviane et al. 1998 for an updated discussion on this subject).

5. Population ratios and radial gradients

Another useful application of the star counts in the different evolutionary phases is the calculation of the population ratios. In particular, here we can use the R-ratio (i.e the ratio of the number of the HB stars to the number of the RGs with bolometric magnitudes brigther than the HB magnitudes: $R = N_{HB}/N_{RGB}$) proposed by Iben (1968) to derive the amount of the original helium in M 80. Table 6 presents the number of stars in the two branches, N_{HB} and N_{RGB}, together with R values for three annuli at different distances from the cluster center and for the "complete" sample (stars with $r > 250$ pix). The HB luminosity level of the RGB was fixed taking into account a differential bolometric correction between HB and RGB stars of 0.15 mag. The uncertainties shown in the Table take into account only the Poisson noise and neglect the errors coming from the uncertainty in the determination of V_{HB} which produces a variation of ± 0.1 in R.

The "complete" sample gives a value of $R = 1.32 \pm 0.30$ in full agreement with the value obtained by Buonanno et al. (1994) for M 3 ($R = 1.35 \pm 0.20$) and, more generally, with those presented by Buzzoni et al. (1983) for a sample of 15 clusters. However, the quoted authors adopt as HB level the mean magnitude of stars in the RR Lyrae gap, while we use the lower envelope of the HB. Following the Buzzoni's approach we would have a slightly higher value of R: $R_{HB,mean} = 1.40 \pm 0.30$ for the "complete" sample.

Table 5. Distance from different calibrations of the magnitude of the ZAHB.

M_V	ΔM_V	(m–M)	Δ(m–M)	author	method
0.43	0.06	15.77	0.12	Sandage 1993	Period Shift
0.66	0.07	15.54	0.12	Buonanno et al. 1989	MS Fit
0.64	0.04	15.56	0.11	this paper	Theoretical
0.75	0.03	15.45	0.10	Carney 1992	Subdwarfs
0.61	0.04	15.59	0.11	Fernley 1994	Baade–Wesselink

Table 6. Number of HB and RGB stars (N_{HB}, N_{RGB}), value of R for the specified annulus. The Table also shows the number of HB stars in the blue tail (N_{BHB}), the number of stars brighter than blue tail stars (N_{RHB}), and the ratios $\tilde{R}$ and R_3 (see text).

r (pix)	N_{HB}	N_{RGB}	R	N_{RHB}	N_{BHB}	$\tilde{R}$	R_3
$100 \div 250$	112	107	1.05 ± 0.20	76	36	0.71 ± 0.15	0.47 ± 0.13
$250 \div 500$	80	41	1.95 ± 0.50	36	44	0.87 ± 0.30	1.22 ± 0.39
> 500	18	33	0.54 ± 0.20	15	3	0.45 ± 0.20	0.20 ± 0.17
> 250	98	74	1.32 ± 0.30	51	47	0.69 ± 0.20	0.91 ± 0.26

Adopting the calibration of Buzzoni et al. for the R-Y relation and the value $R_{HB,mean}$ from the "complete" sample, we have $Y = 0.23 \pm 0.04$; by using a more recent calibration (Bono et al. 1995), which involves the ZAHB level approach, we have (for Z=0.0005) $Y = 0.25 \pm 0.05$, both in agreement with the generally accepted value of Y=0.23. Note that these determinations of Y must be considered as lower limits: our counts are incomplete at the limiting magnitude and we cannot exclude that the blue HB tail continues beyond the limit in our photometry. The problem of the field contamination on the blue HB tail has been investigated. Even if no conclusive results can be derived, we suggest that the blue tail stars belong to the cluster. First, by examining the field stars contribution in this region, as observed in a field located at ~ 30 arcmin from the center of the cluster, we found that no contamination is expected for $V < 20$. Second, some indication can be derived by using stellar population counts.

In this sense, even if affected by a large error, our determination of R allows to add further indication that the stars in the blue tail should be indeed genuine HB members. In fact, considering for example as "HB" only that part of the horizontal branch whose morphology is in common with that of M 3 ($V < 17$), we would have an amount of HB stars as given in column 5 of Table 6 (N_{RHB}) and a consequent value $\tilde{R} = N_{RHB}/N_{RGB} = 0.69 \pm 0.20$ (i.e. $Y \simeq 0.10$) which can hardly be accepted. Of course this method could be biased by any "non-evolutionary" phenomena acting in the way of modifying the ratios between stars in different evolutionary phases.

For the innermost sample ($100 < r < 250$ pix) we derive a smaller value of R, which is probably due to incompleteness of our photometry in a more crowded region of the cluster. Nevertheless, the analysis of the outer (complete) annuli ($250 < r < 500$ pix and $r > 500$ pix) shows the occurrence of a radial gradient in the parameter R, from which one could infer that, moving toward the cluster center, an excess of HB stars and/or a depletion of RGB stars takes place (see Djorgovski & Piotto 1993 for very similar results in other high concentration globular clusters like M 15, M 30, and NGC 6397).

The same Table 6 presents the values for R_3 defined as the ratio N_{BHB}/N_{RHB}, where $N_{BHB} = N_{HB} - N_{RHB}$ is the number of stars in the blue tail ($V > 17$). Again, the values of R_3 for the two outer annuli reveal that the number of BT stars increases toward the cluster center. This appears a significant result, since those stars are fainter and more affected by incompleteness, more severe in the inner regions, than the brighter red horizontal branch (RHB) stars. A similar occurrence was found also in NGC1904 (Ferraro et al. 1992a). For a more significant comparison of the radial distribution of the stars in the different evolutionary phases, we have calculated the cumulative distribution. As shown in Fig. 5 the radial trend of the R and R_3 ratios are due to an increase in the number of the HB stars toward the cluster center (note that we have used only stars with $r > 250pix$, i.e. $r > 87$ arcsec), and not to a dimise of RGB stars. In particular, if we keep the division in RHB ($V < 17$) and blue horizontal branch (BHB) ($17 < V < 20$), a Kolmogorov–Smirnov test shows that the BHB stars are significantly more concentrated (at 99.8% probability level) than the SGB stars (defined as stars within 3 sigma from the fiducial sub–giant branch and with $19 < V < 17$); the RHB stars are more concentrated, but this last result is less significant (Fig. 5, upper panels). The BHB stars are more concentrated (at the same significance level) even if we limit the BHB sample to $17 < V < 19$ or to $17 < V < 18$: not only the result is significant, but we can exclude it is an artifact due to the inclusion of spurious detections, as it could happen extending the counts to the limit of the photometry. Neither the incompleteness can explain the radial trends shown in the upper panels of Fig. 5. On the other side, the RGB stars have exactly the same distribution as the SGB stars (Fig. 5, lower panel).

A similar result has been found in NGC 1851 (Saviane et al. 1998), though at a lower significance level, and also NGC 1904 shows the same effect.

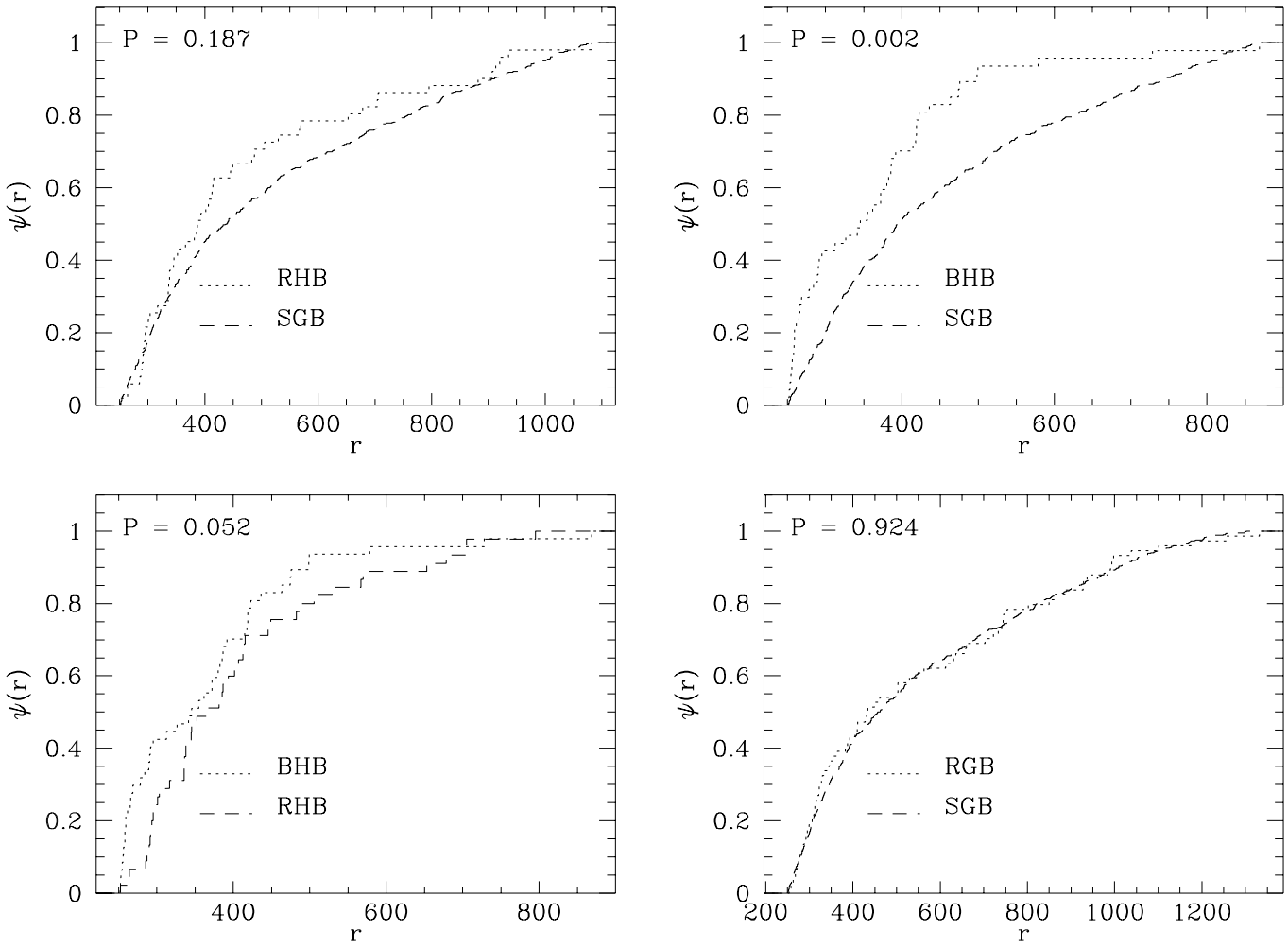

Fig. 5. The cumulative distributions of several star samples are compared with the template SGB stars (see text for the definition). The upper panels show that both BHB and, to a lower extent, RHB stars are more concentrated than SGB stars. The probability that BHB and SGB stars are taken from the same distribution is only 0.2 %. This is confirmed by the lower left panel, which shows that the BHB stars are also more concentrated than the red HB counterpart. Conversely, the lower right panel demonstrates that the RGB stars and SGB stars share the same radial distribution.

Undoubtedly, the most interesting feature in the CMD of Fig. 1 is the prominent blue tail of the HB. Extended blue tails have been found in many other galactic GCs, and their nature and, overall, their origin is not well understood, yet (Sosin et al. 1997). As shown above, whatever the BHB stars are, they must be the natural descendant of the RGB stars, if we exclude anomalous helium content for M 80. However, while the RGB stars have the same distribution of the other fainter stars populating M 80, the BHB stars are significantly more concentrated towards the inner parts of the cluster.

It is hard to interpret this observational evidence, from the dynamical point of view. It cannot be mass segregation, as, interpreting the BHB stars as normal He burning stars, they must be less massive than RGB stars. On the other side, whatever the mechanism responsible of this stellar distribution is, it must be effective far from the cluster core. One possibility is that some of these blue tail HB stars are just stars that, due to some close encounters in the inner high density cores, have lost most of their envelope, and, at the same time, gained enough energy to be ejected from the core to the outer envelope. This mechanism could qualitatively explain the gradients in the BHB stars (the probability of gaining energy is lower for the higher energy corresponding to larger orbits). If this is the case, we would expect an anomalously high R ratio. The fact that the R ratio 'seems' normal can be explained by the fact that we do not count all the BHB stars, as the blue tail extends beyond the limit of our photometry. This attempt of explanation cannot be more than a simple speculation till we will be able to map the entire cluster from the inner core to the outer envelope to better track the stellar distribution. Calculation of the cross section for encounters able to strip part of the envelope and to leave the star with a higher energy would be most valuable. Whatever the interpretation of these results is, these features suggest the occurrence of local modifications in the stellar populations of the cluster in agreement with what is found in other dense and post-core-collapse

globulars (see e.g. Djorgovski & Piotto 1993, Djorgovski et al. 1991, Castellani 1994, Fusi Pecci et al. 1993).

6. Comparison with other clusters.

As largely debated in recent literature, the direct comparison of the CMDs of clusters with similar metallicity is the safest way to deal with many fundamental problems, e.g. possible age differences among clusters with similar metallicity.

In this respect let us first address a methodological warning. As a matter of fact, in the literature, many discussions on the argument are based on the evaluation of selected values, like the turn-off luminosity or the HB luminosity level. However, one knows that similar parameters do depend on difficult evaluations and sometimes on subjective estimates, thus containing more or less relevant errors. On the other hand, the observational CMD is the only real experimental data set one is dealing with. To substantiate this warning, let us only recall one evidence: the group of very metal poor galactic globulars has been described as having indistinguishable CMDs (see e.g. Richer, Fahlman & Vandenberg 1988, Vandenberg, Bolte & Stetson 1990). In spite of such a direct evidence, there are compilations scattered in the literature (see. e.g. Chaboyer & Kim 1995) for which these clusters should have a spread in the differences between the HB and TO luminosity, and thus different ages. According to such an evidence and in order to avoid unnecessary (and dangerous) approximations, the analysis presented below will be always based on the comparison of the original CMDs, even if in this paper we will be forced to use ridge lines for the sake of typographical clarity.

According to theoretical predictions, in old clusters with similar heavy elements abundances MS, RGB and HB should have the same color–magnitude location, with TO location marking differences in age, if any. In the case of M 80, the natural candidates for such a comparison are NGC 1904, NGC 5272 (M 3), NGC 5897, NGC 6205 (M 13), NGC 6218 (M12), and NGC 7492, clusters which have the same [Fe/H] within ± 0.1 dex.

Fig. 6 displays a comparison of the CMD of M 80 with the CMDs for some of these clusters, i.e. M 3 (Ferraro et al. 1997), M 13 (Paltrinieri et al. 1997), NGC 7492 (Buonanno et al. 1987). They show a reasonable good agreement at least as far as the location of the luminous RGB and HB stars is concerned. On the other hand, Fig. 7 shows the comparison of the CMDs for another set of clusters: M 80 (this paper), NGC 1904 (Ferraro et al. 1992a), M12 (Brocato et al. 1996), NGC 5897 (Ferraro et al. 1992b). Even a quick inspection of Fig. 7, discloses serious problems. Assuming a common magnitude for their HBs, the overlap of the their RGBs produces a discrepancy in the blue HB distribution (upper panel). On the other hand, one finds that all the HBs can be nicely overlapped, provided that a significant difference in the RGBs is accepted, with M12 branch appearing sensitively redder than that of M 80 (lower panel). In Fig. 8 we show a direct comparison of our M 80 CMD with the fiducial sequence of M12, i.e the two clusters which represent the extremes in the previous comparison.

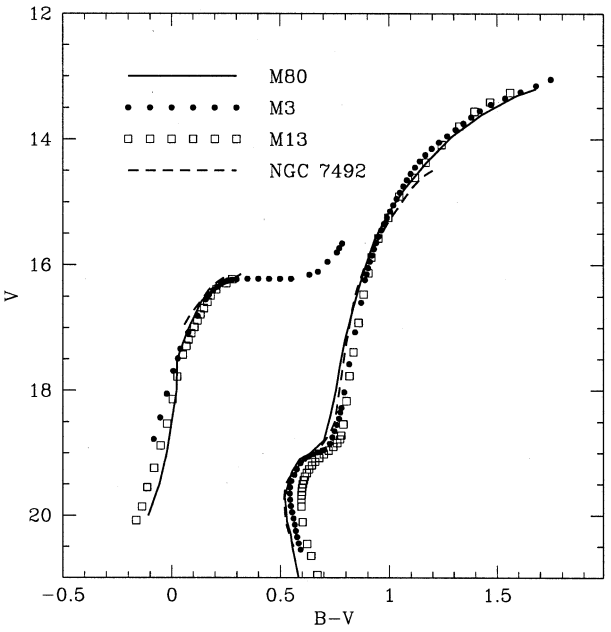

Fig. 6. Comparison of the fiducial lines of M 80, M 3, M 13, and NGC 7492.

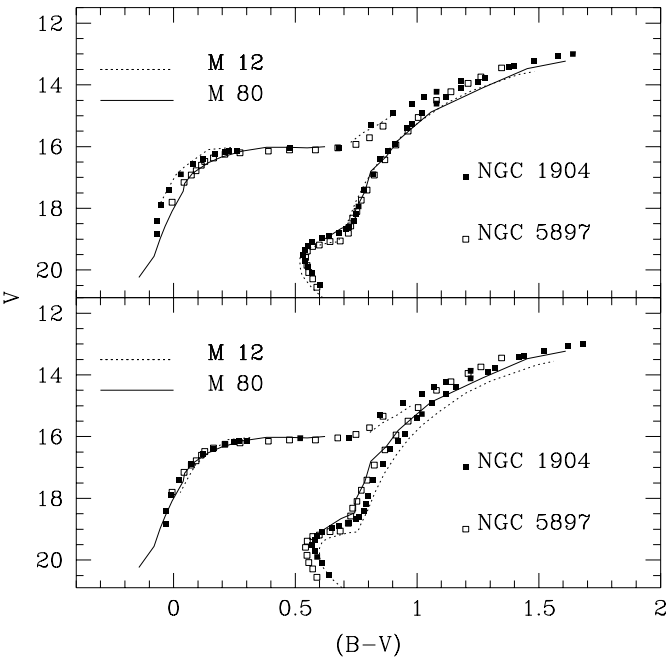

Fig. 7. Comparison of the fiducial lines of M 80 with M12, NGC 1904, and NGC 5897. The fiducial lines have been normalized at the TO (*upper panel* and at the HB-TD (*lower panel*).

Let us try to discuss a little bit in detail the possible origin of this discrepancy. Many causes can be responsible for the detected differences, e.g. calibration errors, age, and metallicity differences. In the following we will analyse some of them:

• *calibration errors*

The most natural explanation for such an occurrence is that something was wrong in the color calibration, either in our or in

the data taken from the literature. The errors in the photometric calibration might produce a spread in the relative position of the different branches in the CMD, though a spread of 0.1 magnitudes in a range of 0.6-0.9 magnitudes in (B-V) would imply an error of $> 100\%$ in the slopes of the calibration curves from the instrumental to the standard magnitudes, quite unlikely in the CCD era but not unusual if photometric sequences based on photographic data have been used as 'calibrators'.

In this respect the case of M 3 is emblematic: the new photometric calibration recently published by Ferraro et al. 1997, based on Landolt (1992) standard stars has been found to show large systematic differences (at a level of ~ 0.1 mag) with respect to the previous photometry by Buonanno et al. (1994) based on the original calibration by Sandage (1970). The same result has been found in M 13 by Paltrinieri et al. (1997). In the latter paper the authors emphasize that the photometry calibrated on photographic sequences may be affected by strong color terms. In some cases (as in M 13) the color differences have been found to be strongly dependent on the magnitude, with effects on the morphology of the main branches in the CMD. As a matter of fact, there is no large sample of observationally (same telescope, filters, calibrations, adopted standard stars etc) homogeneous CMDs representing the galactic globular cluster system. This may play a role in comparing CMDs of different clusters.

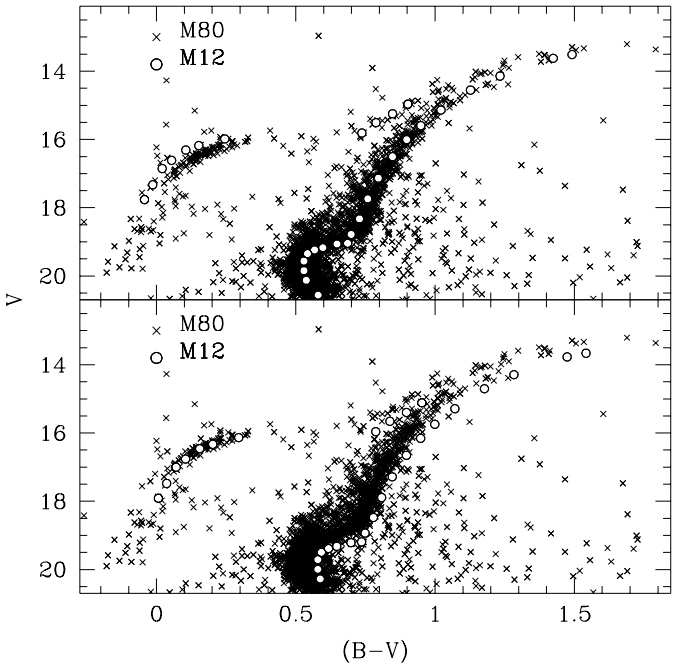

Fig. 8. Comparison of the fiducial lines of M12 with the observed CMD of M 80. Two different normalizations are shown in the two panels. None gives a satisfactory overlap.

• *age differences*

We already mentioned that clusters with similar metallicities should have similar CMD locations for all the evolutionary phases, but the TO. To enter into details, such clusters are expected with nearly identical MSs and the RGBs only slightly moving toward the red as the cluster age increases. Quantitatively, one finds that at the luminosity of the HB the RGB becomes redder by about $\Delta(B-V) \simeq 0.01$ when passing from 12 to 16 Gyr, with a further reduced dependence on age for larger ages.

Bearing in mind such a theoretical scenario, by playing with cluster reddenings and distance moduli one can produce a relative location of the TO regions in the two clusters as expected if M12 is older (by about 2-3 Gyr) than M 80. However, Fig. 8 (upper panel) shows that under these assumptions the HB locations disagree in a way not supported by any theoretical prediction.

One can perform a much more reasonable comparison by observing that the turn down of the HB luminosity at the larger temperatures (HB-TD) should be largely unaffected both by the cluster age and by the cluster metallicity. For what concerns the first statement, we note that the age affects the ZAHB sequences of a given chemical composition through variation in the mass of the He core (M_c) at the He ignition. From Sweigart & Gross (1976) results one obtains for ZAHB models in the RR Lyrae region (but the dependence on T_e is negligible): $d \log L_{ZAHB}/dM_c \simeq 3.4$. Furthermore, from Straniero & Chieffi (1991) one derives a variation of $\Delta M_c \simeq 0.002 M_\odot$ in the core mass at the He flash for models of given [Fe/H]=-1.7 passing from an age of 12 Gyr to 16 Gyr. This means that only a variation of $\Delta \log L_{ZAHB} \simeq 0.007$ is expected in this case.

• *metallicity differences*

Fig. 9 shows the theoretical prediction for the CMDs for the given labeled age but for a cluster metallicity spanning the range Z= 0.0001-0.001. As an important point, one finds that, whereas the RGB and – to a less extent – the MS depend on the metallicity, the HB-TD appears independent of such a parameter. This is the consequence of the small dependence of the HB luminosity on metallicity and of the evidence that *the HB-TD is a temperature indicator, marking the effective temperature where bolometric corrections start sensitively affecting the V magnitude*. On the basis of theoretical evaluations presented by Bono et al. (1995) one can add the further evidence that both the HB-TD and the RGB are fairly independent of the assumed amount of original He.

As a whole, one derives the theoretical evidence that the HB-TD is the only observational parameter whose CMD location is expected on theoretical ground to remain reasonably fixed when varying cluster ages and/or metallicities and/or the amount of the original He. That is, the HB-TD appears an useful observational parameter to reasonably compare the CMD of different clusters. According to such an evidence, one concludes that the more meaningful comparison between M 80 and M12 should be just the one already reported in the lower panel of Fig. 8. By comparing the relative location in that figure with the theoretical predictions given in Fig. 9, one finds that the differences between the two clusters are just the ones expected if M12 is more metal rich than M 80. As an important point, Fig. 8 shows that in this case both clusters do not show a clear difference in age, differences in the turn-off distributions being expected as a consequence of the difference in metallicity.

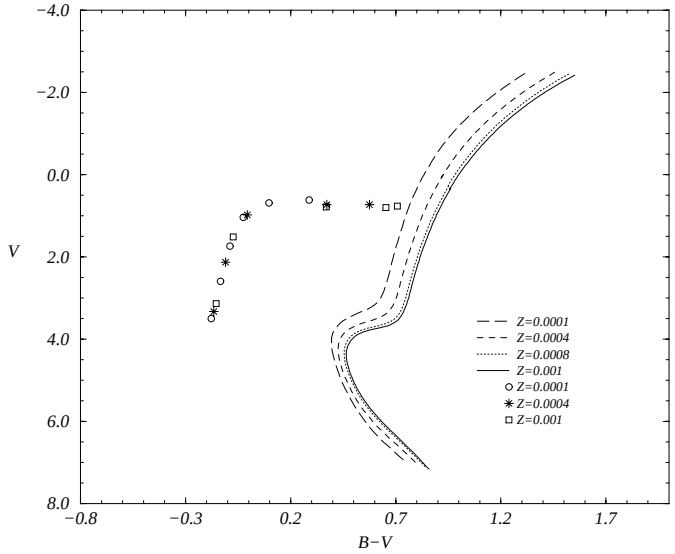

Fig. 9. H-burning isochrones as in the previous figure but for a fixed age of 16 Gyr and for various values of the metallicity (lines). Theoretical ZAHBs for three choices of the metallicity from Castellani et al. 1991 (symbols).

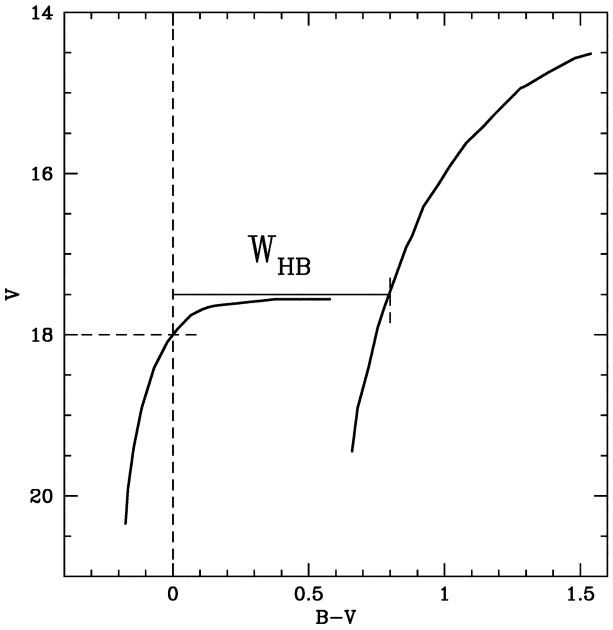

Fig. 10. The fiducial line of NGC 1904 used as reference; the W_{HB} is also shown.

In the following we will adopt the metallicity scale defined by Zinn (Zinn & West 1984, Zinn 1985), though a new scale has been recently proposed by Carretta & Gratton (1997). This scale has been obtained from direct measurements of the Fe lines in high resolution spectra of a sample of giants in each cluster. In general the Carretta & Gratton (1997) scale assigns higher metallicity (~ 0.2 dex) with respect to Zinn scale, but the relation between the two scales is not linear (see Carretta & Gratton 1997 for a discussion). Another important point that deserves attention in defining the metallicity of a cluster is the abundance of the so-called α-elements (O, Ne, Mg, Si, S, Ca). As stated by Renzini (1977), the location of the RGB in the CMD is mainly driven by the abundance of the low-ionization potential elements (mainly Mg, Si and Fe). Moreover, as noted more than 10 years ago by Geisler (1984), the observed $(B-V)$ color of the RGBs of the GGCs correlates better with $[(Mg+Si+Fe)/H]$ than with [Fe/H] (cf. also Salaris & Cassisi 1996). So the α-elements abundance plays a fundamental role in this play.

It is now generally accepted that α-elements are overabundant with respect to iron in GGCs (e.g. Gratton 1987); on the other hand, direct measures of the α-element abundances have been obtained, up to now, only for an admittedly small sample of GGCs (see Table 2 by Carney 1996 and Table 1 by Salaris & Cassisi 1996). Salaris, Chieffi and Straniero (1993) have investigated the influence of the α-elements on the evolution of low mass stars and concluded that α-enhanced ishocrones are mimicked by standard scaled solar isochrones of corresponding global metallicity $[M/H]$ given by:

$$[M/H] = [Fe/H] + Log(0.638 f_\alpha + 0.362)$$

where f_α is the enhancement factor.

In this scenario the detected differences shown in Fig. 7 could derive from similar abundances in [Fe/H], but different values of global metallicity ($[M/H]$) reflecting different abundances of the α elements present in different clusters.

The behavior discussed above, prompted us to compare the CMDs of M12 and M 80 with other Galactic halo clusters. We selected a sample of intermediate-low metallicity clusters for which the list with magnitudes and positions were available in electronic form. The references of the selected data base is listed in the caption of Fig. 11. To provide a quantitative description, we have approached the problem as follows. We have devised a new parameter (W_{HB}) to measure the distance (in color) between the HB-TD and the RGB: we fixed the HB-TD at $(B-V)_0 = 0$ and measured the RGB color at 0.5 magnitudes brighter than the HB-TD level. As the position of the HB turn down is fixed, W_{HB} just shows the displacement of the RGB as a function of the metal content. Fig. 10 show the parameter W_{HB} for the mean ridge line of NGC 1904 (Ferraro et al. 1992a) which has been used for reference.

Fig. 11 shows W_{HB} as a function of the metallicity for the selected sample of clusters. The trend with the metallicity is clear, and in the direction expected from the theoretical models. The *dashed line* shows the expected value of W_{HB} from Straniero and Chieffi (1991) models. The general trend of the points is the one expected from the models, though we note a large dispersion, which is particularly evident at intermediate metallicity ($-1.85 <$[Fe/H]< -1.50), slightly larger than expected on the basis of the measurement errors. This dispersion can be interpreted simply as a spread in the values W_{HB} due to measurement and calibration errors, or in terms of a real (physical) dispersion. As suggested above, the abundances of α elements can play an important role in increasing the dispersion in Fig. 10, for this reason the direct determination of the

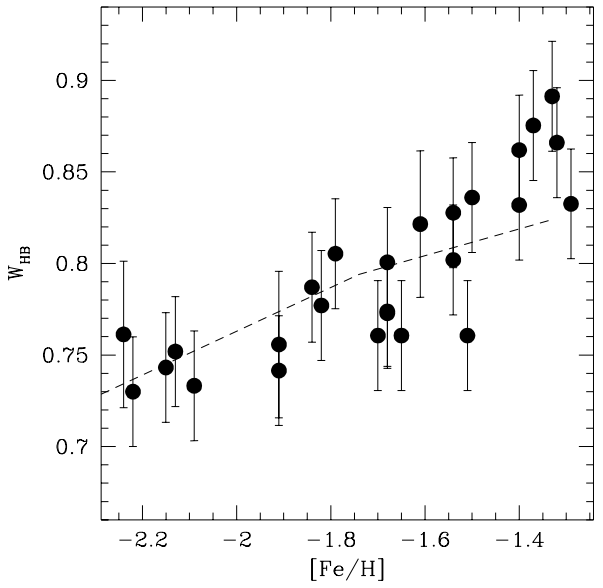

Fig. 11. The W_{HB} is plotted against the metallicity for 26 globular clusters. The dotted line represents the expected trend of W_{HB} from the Straniero and Chieffi (1991) models. The objects we have used are: NGC288: (Bergbusch 1993), NGC1261 (Ferraro et al. 1993), NGC1851 (Walker 1992), NGC1904 (Ferraro et al.1992a), NGC2808 (Ferraro et al. 1990), NGC4590 (Walker 1994) IC4499: (Ferraro et al.1995), NGC 5272 (Ferraro et al. 1997) NGC 5286, NGC 6218, NGC6717, NGC6981 (Brocato et al. 1996), NGC5466 (Buonanno et al. 1984), NGC5694 (Ortolani and Gratton 1990), NGC5897 (Ferraro et al. 1992b), NGC 5904 (Sandquist et al. 1996), NGC 6093 (this paper), NGC 6205 (Paltrinieri et al. 1997), NGC6341 (Carney et al. 1992), NGC 6397 (Kaluzny et al. 1997), NGC6584 (Sarajedini and Forrester 1995), NGC 6809 (Desidera 1996), NGC7078 (Durrel and Harris 1993), NGC 7099 (Bergbush 1996), NGC7492 (Buonanno et al. 1987), Arp 2 (Buonanno et al. 1995).

α elements for an extensive sample of GGCs is fundamental in order to shed light into this problem.

To summarize, the possibility given by modern computing technique to directly compare the CMDs presented in the literature brings to the light the evidence that over a very large range of (nominal) metallicities the difference in color between the HB-TD and the RGB in the CMDs of galactic globular clusters appears to follow the general trend predicted by the theoretical models, but with a large spread.

Such an evidence might simply be the consequence of the errors in the photometry calibration, as already quoted in the previous paragraph. But if observational errors are not the main responsible for the distribution shown in Fig. 11, the field is obviously open to discussions and investigations. We have shown that cluster ages can hardly play a role in this scenario, while it is possible that the observed distribution reflects a peculiar distribution in the global metallicity of the clusters. Direct measures of α elements are urged to better understand the observed behaviour.

Let us to close the paper without entering in further details, since, in our feeling, the actual priority is to test whether or not the presented scenario will survive to further investigations. If this will be the case, this will of course open a series of related questions about the history of the galactic halo.

Acknowledgements. The authors wish to thank Simone Zaggia for help during the observations. We warmly thank S. Cassisi, A. Piersimoni and G. Raimondo for a careful reading of the manuscript.

References

Bergbusch P.A., 1993, AJ 106, 1024.
Bergbusch P.A., 1996, AJ 112, 1061.
Bica E.L.D., Pastoriza M.G., 1983, Ap&SS 91, 99.
Bono G., Castellani V., Degl'Innocenti S., Pulone, L., 1995, A&A 297, 115.
Brocato E., Buonanno R., Malakhova Y., Piersimoni A.M., 1996, A&A 311, 778.
Brodie J.P., Hanes D.A., 1986, ApJ 300, 258.
Buonanno R., Buscema G., Corsi C.E., Ferraro I., Iannicola G. , 1983, A&A 126, 278.
Buonanno R., Buscema G., Corsi C.E., Iannicola G., Fusi Pecci F., 1984, A&ASS, 56, 79,
Buonanno R., Corsi C.E., Bellazzini M., Ferraro F.R., Fusi Pecci F., 1997, AJ 113, 706.
Buonanno R., Corsi C.E., Fusi Pecci F., 1985, A&A, 145, 97.
Buonanno R. Corsi, C.E., De Biase G.A., Ferraro I., 1979, in: International Workshop on Image Processing in Astronomy, p. 354, eds. G. Sedmak, M. Capaccioli & R.J. Allen, ICTP, Trieste, Italy.
Buonanno R., Corsi C.E., Buzzoni A., Cacciari C., Ferraro F.R., Fusi Pecci F., 1994, A&A 290, 69.
Buonanno R., Corsi C.E., Ferraro I., Fusi Pecci F., 1987, A&A suppl. 67, 327.
Buzzoni A., Fusi Pecci F., Buonanno R., Corsi C.E., 1983, A&A 123, 94.
Caloi V., Castellani V., Cassatella A., Ponz D., in Proceedings of 2nd Europen IUE Conference, Tübigen, Germany, 26-28 March 1980, p. 179 (ESA SP-157, April 1980).
Caloi V., Castellani V., Galluccio D., in Proceedings of 4th Europen IUE Conference, Rome, Italy, 15-18 May 1984, p.497, ESA.
Caputo F., 1997, MNRAS, 284, 994
Carney, B.W. 1996, PASP, 108, 900.
Carney B.W, Storm J., Beck J.A., 1991, PASP. 103, 1264.
Carney B., Storm J., Trammell S.R., Jones R.V., 1992, PASP 104, 44.
Carretta E. , Gratton R.G., 1997, A&ASS 121, 95.
Castellani V., 1994, Mem. Soc. Astron. It. 65, 649.
Castellani V., Chieffi A., Pulone L., 1991, ApJS 79, 911 (CCP).
Castellani V., Degl'Innocenti S., Pulone L., 1995, ApJ 446, 228.
Chaboyer B. & Kim Y-C 1995, ApJ 454, 767.
Degl'Innocenti S., Weiss A., Leone L., 1997, A&A, 319, 487
Desidera, S. 1996, Master thesis, Univ. Padova.
Djorgovski S. 1993, PASPC 50, 373.
Djorgovski S. & Piotto G., 1992, AJ 104, 2112.
Djorgovski S., Piotto G. 1993, PASPC 50, 203.
Djorgovski S., Piotto G., Phinney E.S., Chernoff D.F., 1991, ApJ, 372, L41.
Durrell P. R. & Harris W. E., 1993, AJ 105, 105.
Ferraro F.R., Carretta C., Corsi C.E., Fusi Pecci F., Cacciari C., Buonanno R., Paltrinieri B., Hamilton D., 1997, A&A 320,757.
Ferraro F.R., Clementini G., Fusi Pecci F., Buonanno R., Alcaino G., 1990, A&AS 84, 59.
Ferraro F.R., Clementini G., Fusi Pecci F., Sortino R., Buonanno R., 1992a, MNRAS 256, 391.

Ferraro F.R., Clementini G., Fusi Pecci F., Vitiello E., Buonanno R. 1993, MNRAS 264, 273,
Ferraro I., Ferraro F.R, Fusi Pecci F., Corsi C.E., Buonanno R., 1995, MNRAS 275, 1057.
Ferraro F.R., Fusi Pecci F., Buonanno R., 1992b, MNRAS 256, 376.
Fusi Pecci F., Ferraro F.R., Crocker D.A., Rood R.T., Buonanno R., 1990, A&A 238, 95.
Fusi Pecci F., Ferraro F.R., Bellazzini M., Djorgovski S., Piotto G., Buonanno R., 1993, AJ, 105, 1145.
Geisler D. 1984, ApJ, 287, L85.
Gratton R.G., 1987, A&A 179, 181.
Harris W.E. & Racine R., 1974, AJ 79, 472 (HR74).
Hartwick F.D.A., 1968, ApJ 154, 475.
Iben Jr. I., 1968, Nature 220, 143.
Kaluzny et al. 1997, in press.
Kurucz, R., in IAU Symp. n 149, "The Stellar Populations of Galaxies" ed. B. Barbuy, A. Renzini, (Dordrecht:Kluwer), p.225 (1992).
Landolt A.U., 1983, AJ, 88, 439.
Ortolani S., Gratton, R., 1990, A&AS 82, 71.
Paltrinieri B., Ferraro F.R., Fusi Pecci F., Carretta E., 1998, MNRAS 293, 434
Racine R., 1973, AJ 78, 180.
Reed B.C., Hesser J.E.& Shawl S.J., 1988, PASP. 100, 545.
Renzini, A. 1977, in Advanced Stages in Stellar Evolution, edited by P. Bouvier and A. Maeder, (Geneva Observatory), p. 149.
Richer H.B., Fahlman G.F. & Vandenberg D.A. 1988, ApJ 239, 187.
Salaris M., Cassisi S, 1996, A&A 305, 858.
Salaris M., Chieffi A., Straniero O. 1993, ApJ 414, 580.
Salaris M., Degl'Innocenti S., Weiss A., 1997, ApJ, 479, 665
Sandage A. 1970, ApJ, 162, 841.
Sandage A.R. & Smith L.L., 1966, ApJ 144, 886.
Sandage A.R. & Wallerstein G., 1960, ApJ 131, 598.
Sandquist E.L., Bolte M., Stetson P.B., Hesser J.E., 1996, AJ 470, 910.
Sarajedini A., Norris J.E. 1994, ApJS 93, 161.
Sarajedini A., Forrester W.L., 1995, AJ 109, 1112.
Saviane I., Piotto G., 1998, in preparation.
Saviane I., Piotto G., Fagotto, F., Zaggia, S., Capaccioli, M., and Aparicio A. 1998, A&A 333, 479
Shara, M.M., Drissen, L. 1995, ApJ, 448, 203.
Sosin C., et al., 1977, ApJ, 484, L25.
Sweigart A.V. & Gross P.G., 1976, ApJ 32, 367.
Straniero O. & Chieffi A., 1991, ApJS 76, 525.
Suntzeff N.B., Kinmann T.D. & Kraft R.P., 1991, ApJ 367, 528.
Vandenberg D.A., Bolte M. & Stetson P.B. 1990, ApJ 100, 445.
Walker A.R., 1992, PASP 104, 1063.
Walker A.R., 1994, AJ 108, 555.
Wehlau A., Sawyer Hogg H. & Butterworth S., 1990, AJ 99, 1159.
Zinn R. & West M.J., 1984, ApJS 55, 45.
Zinn, R., 1985, ApJ 293, 424.